

COMPUTATIONAL NEUROIMAGING OF HUMAN VISUAL CORTEX

Brian A. Wandell

Neuroscience Program and Department of Psychology, Stanford University, Stanford, California 94305; e-mail: wandell@stanford.edu

KEY WORDS: fMRI, visual cortex, motion, color, behavior, dyslexia

ABSTRACT

Functional magnetic resonance imaging is a new neuroimaging method for probing the intact, alert, human brain. With this tool, brain activity that has been hidden can now be measured. Recent advances in measuring and understanding human neural responses underlying motion, color, and pattern perception are reviewed. In individual human brains, we can now identify the positions of several retinotopically organized visual areas; measure retinotopic organization within these areas; identify the location of a motion-sensitive region in individual brains; measure responses associated with contrast, color, and motion; and measure effects of attentional modulation on visually evoked responses. By framing experiments and analyses as questions about visual computation, these neuroimaging measurements can be coupled closely with those from other basic vision-science methods.

INTRODUCTION

In his monumental work on visual perception, a work that has remained relevant to vision scientists for more than 100 years, von Helmholtz (1866) suggested how to think about the problem of vision. What we see, he wrote, is the solution to a computational problem. Starting with the light absorbed within our eyes, “such objects are always imagined as being present in the field of vision as would have to be there in order to produce the same impression on the nervous mechanism.” Von Helmholtz frames vision as a computational problem: Given the photon absorptions within our eyes, how do we compute the most likely cause? In some cases, the solution may be unique, so that only a single object

could explain the sensory data. In other cases, the computational solution is underdetermined, so that we must rely on our experience—or the experience in our genes—to select the perception that we imagine.

Von Helmholtz's framing remains a key idea that integrates the many techniques used by vision scientists. The separate disciplines within vision science all contribute to and benefit from thinking of vision as a computational problem. For example, the computational nature of perception is revealed by many of the visual illusions we use to introduce our field. Illusions demonstrate that what we see are not direct measurements of the image but rather interpretations, and important illusions tell us something about the nature of these computations. Also, any account of the visual pathways, from single-unit functional properties to anatomical interconnections, are most meaningful when we understand how they explain the visual computations of motion, pattern, and color (Hubel 1988, Wandell 1995). Significant insights into computational processing have also been obtained by studying individuals who have lost a portion of their brain, or who were raised without the opportunity for vision to develop normally (Gregory 1974, Zeki 1993). And finally, many insights into the nature of visual computation itself have been derived from the work of individuals who build computational devices to perform visual tasks (Marr 1982).

This review poses a question: How can neuroimaging results be integrated into the fundamental computational framework of vision science? To answer the question, I review recent advances in measuring and understanding the neural basis of visual computation in the human brain. The review mainly covers measurements made using a relatively new technique, functional magnetic resonance imaging (fMRI).

It has been seven years since the first measurements of fMRI signals from human cortex were reported (Kwong et al 1992, Ogawa et al 1992). In that short time, much progress has been made in both measurements and analysis of visually driven activity. In individual human brains, we can now identify the positions of several retinotopically organized visual areas; measure retinotopic organization within these areas; identify the location of a motion-sensitive region in individual brains; measure responses associated with contrast, color, and motion; measure localized deficits in activity in subjects with cortical damage; and measure effects of attentional modulation on visually evoked responses. Some of these measurements have important precedents in the positron emission tomography (PET) literature, but the signal-to-noise ratio (SNR) of fMRI is superior and provides better spatial localization. Finally, the accessibility of magnetic resonance scanners has greatly expanded the number of research groups contributing to neuroimaging, and this has brought with it vitality and new ideas.

After reviewing the results, I take stock of how fMRI technology has changed the experimental neuroimaging questions we ask and the analytic methods we

use. Prior to fMRI, neuroimaging primarily tested hypotheses about the localization of function by asking whether two stimuli (or tasks) caused statistically different signals within the brain. The SNR of fMRI is large enough to measure the size of differences, not just their presence or absence. For this reason, hypotheses about neural computations, beyond localization, can be framed and tested. Hence, fMRI opens up a new array of questions and has initiated an era of computational neuroimaging. In this spirit, this review emphasizes that portion of the recent visual neuroimaging literature that addresses computational questions.

THE fMRI SIGNAL

The Biological Source of the fMRI Signal

The fMRI signal is an indirect measure of neural activity that measures changes in the local blood oxygenation level (Moseley & Glover 1995). The indirect nature of the fMRI signal is illustrated in Figure 1. In a control condition, arteries supply nearly 100% oxygenated blood and roughly 40% of the oxygen is consumed locally, so that the blood returning in the veins comprises 60% oxygenated and 40% deoxygenated blood. When a stimulus causes significant neural activity, an additional supply of oxygenated blood is delivered, but not all of the incremental supply is metabolized. Because the fraction of extracted oxygen is reduced compared with the control state, the proportion of oxygenated to deoxygenated blood becomes, say, 63:37. The change in the ratio of oxygenated to deoxygenated blood alters the local magnetic field and this can be detected in the MR signal. This signaling mechanism is the blood oxygen level-dependent (BOLD) signal.¹

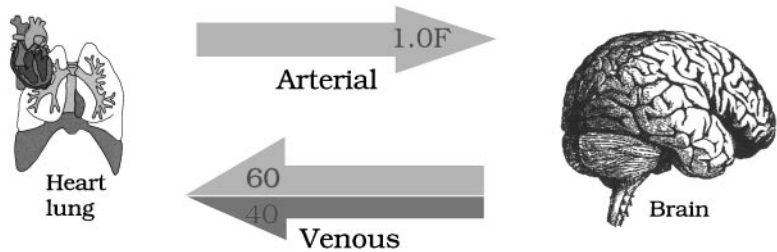
The first reports of BOLD fMRI activity caused widespread excitement in the scientific community in general. Within the smaller community of neuroimaging scientists, the reports raised two important questions: What neural signals are responsible for controlling the vascular changes, and which elements of the vasculature provide the main source of the BOLD fMRI signals?

Neural Control Signals

Understanding the neural control signals will be a great help in interpreting the fMRI signal and relating the measurements to single-unit observations. There

¹Fox & Raichle (1986) and Fox et al (1988) suggested that the mismatch between the incremental blood supply and the incremental metabolism arises because the two systems are only loosely coupled. Buxton & Frank (1997) suggest that given certain basic considerations about the flow of oxygenated blood, the difference is to be expected even if delivery and metabolism are closely linked. It is important to decide this issue in order to understand whether or not the BOLD signal is a precise and reliable estimator of the neural activity.

(A) Control state



(B) Active state

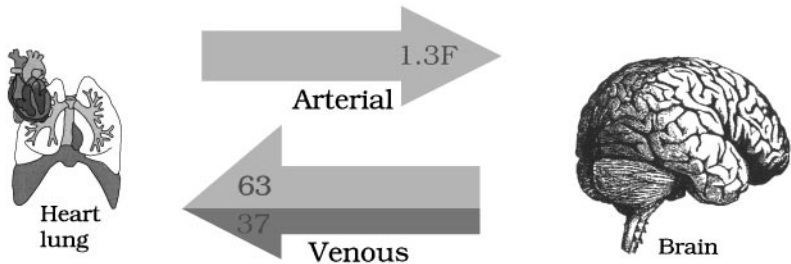


Figure 1 Functional magnetic resonance imaging measures activity-dependent changes in blood oxygenation. (A) In the control state, the arterial supply is fully oxygenated and the flow rate is F . Roughly 40% of the oxygen is metabolized, so that the ratio of oxygenated-to-deoxygenated blood in the venous is roughly 60:40. (B) In the active state, the arterial flow increases, in this example by 30%. The brain oxygen consumption increases, but by a smaller amount. Hence, the proportion of oxygen in the venous return increases. Because oxygenated blood (HbO_2) is magnetically transparent (diamagnetic), whereas deoxygenated blood (Hb) is not transparent (paramagnetic), differences in the ratio between HbO_2 and Hb can be detected in a magnetic resonance scanner.

are several significant questions about the neural signals that control the vascular response measured by fMRI, including (a) whether excitatory and inhibitory activity influence the fMRI signal in similar ways, and (b) whether simultaneous excitation and inhibition at a single cell, resulting in no action potentials, may nonetheless cause an increase in metabolic and vascular response.

Intrinsic optical imaging is a promising method for analyzing some of these questions about the BOLD fMRI signal (Bonhoeffer & Grinvald 1996). In this procedure, the surface of an animal's brain is exposed, and changes in the cortical surface reflectance are measured while the animal views visual stimuli. The cortical reflectance changes are comprised of several components that can be

separated by their wavelength composition (Malonek & Grinvald 1996). Reflectance changes of the slowly developing component (2s) occur at the same wavelengths as the spectral differences between oxy- and deoxyhemoglobin, so that this component of the intrinsic optical signal may have a common basis with the BOLD fMRI signal. Further studies using this method may clarify the relationship between the vascular response and various neural signals because both neural and optical signals can be measured simultaneously in animal experiments.

Spatiotemporal Resolution of the fMRI Signal

Another important question is whether the BOLD signals arise only from relatively large blood vessels, or whether they arise also from the fine vascular mesh called parenchyma. Identifying the vascular source of the BOLD signals is important because oxygenation levels in large veins reflects activity pooled over large brain regions. Hence, if the BOLD signals arise only from large vessels, the neural resolution of the method could be poor despite the high resolution of the MR signal. Informally, this issue was called the brain-vein debate.

To a large degree, this question has been answered by measurements that probe the spatiotemporal resolution of the fMRI signal. These measurements exploit the retinotopic organization of visual cortex using variants of the methods described in the next section. Here, I summarize the conclusions of these measurements.

First, in retinotopically organized cortex, the fMRI signal changes position smoothly rather than jumping discretely between large veins. Hence, in this portion of cortex, the BOLD signal appears to arise from small as well as large veins. We do not yet know whether this observation will generalize to other parts of the brain (e.g. Lai et al 1993).

Second, using 1.5T magnets, it is possible (*a*) to distinguish reliably between activations separated by less than 1.5 mm in cortex, and (*b*) to resolve spatial variation of the response of 1.1 cycles/cm of cortex (Engel et al 1997a). The first finding shows that fMRI localization is slightly too low to measure certain columnar structures, such as the ocular dominance columns in primary visual cortex. The second finding shows that the responding vasculature drains from cortical regions that span significantly less than a centimeter. Measures of spatial resolution are limited by the signal-to-noise ratio (SNR) of the measurement procedures and apparatus. Current measurements represent only a worst-case bound, and it is possible that the vasculature will reveal finer signals as the instrumentation and procedures improve.

Third, Boynton et al (1996) measured the temporal response of the fMRI signal in calcarine cortex. They modeled the fMRI signal as comprising an

instantaneous nonlinearity that transforms image contrast to a neural response, followed by a linear temporal filter associated with the sluggish vasculature. From measurements using several simple stimuli, they estimated that the temporal filter has a constant delay of roughly 2.5 s and then slowly rises to a peak, roughly 3 s later.

In summary, the spatial and temporal resolution measurements show that in visual cortex, the signal reflects activity localized within a few millimeters of space and a few seconds of time. This resolution has proven sufficient to answer important questions about the organization of human visual cortex. In the following, results concerning retinotopy, visual area identification, motion and color responses, and behavioral correlations are reviewed.

VISUAL AREAS

Over the last 30 years, our understanding of monkey visual cortex has been revolutionized by the identification and analysis of a set of roughly 30 visual areas (Zeki 1969, Van Essen & Zeki 1978, Felleman & Van Essen 1991). Along with single-units and columnar architecture, visual areas define a fundamental spatial scale of brain computation.

In monkeys, visual areas have been defined using a variety of criteria, including (a) anatomical connections, (b) the stimulus selectivity of single-unit responses, (c) architectural properties (e.g. columnar and immunohistochemistry), and (d) retinotopic organization. Most of the methods used in monkeys cannot be used in humans. However, with fMRI it is possible to use retinotopic organization to identify and characterize several human visual areas.

Noninvasively identifying the visual areas in the human brain is important for three reasons. First, the visual areas are an important part of brain organization, and a complete understanding of visual computations must include an explanation of how the computations are segregated with respect to these structures. Second, visual area measurements provide an important link between the last two decades of animal studies and human fMRI studies. The close agreement between these measurements show that the monkey studies provide an excellent model for many features of human cortex and, conversely, that fMRI measurements can contribute to the ongoing analyses of computations in visual cortex. Third, the visual areas represent an important anatomical and functional coordinate frame for identifying locations within cortex. After mapping the visual areas in an observer's brain once, it is possible to describe subsequent measurements of cortical stimulus selectivity with respect to the functional coordinate frame of visual areas. In this way, activity can be accurately compared across observers, even when their physical brain sizes and shapes differ.

Retinotopic Organization of Visual Areas

Within each hemisphere, human area V1 occupies a roughly 4- by 8-cm area located at the posterior pole of the brain in the occipital lobe. A large fraction of area V1 falls in the calcarine sulcus (Figure 2). Studies of patients with localized cortical damage showed that the receptive fields of neurons within area V1 are retinotopically organized (Holmes 1918, 1944; Horton & Hoyt 1991). From posterior to anterior cortex, the visual field representation shifts from the center (fovea) to the periphery. This dimension of retinotopic organization is commonly referred to as eccentricity.

Because of the retinotopic organization of primary visual cortex (V1) and several nearby areas (V2 and V3), it is possible to create stimuli that control the location of the neural activity. Figure 3A represents a flickering ring that contracts slowly from the periphery to the center of the visual field. When the ring reaches the center of the viewing aperture, it is replaced by a new ring at the edge of the display. This contracting ring stimulus creates a traveling wave of neural activity that spreads from anterior to posterior cortex, along the eccentricity dimension. The activity spans several adjacent visual areas, including V2 and V3, that share a similar retinotopic organization with respect to eccentricity. (The ability to control the spatial position of the neural activity was used to make the spatial resolution measurements described earlier.)

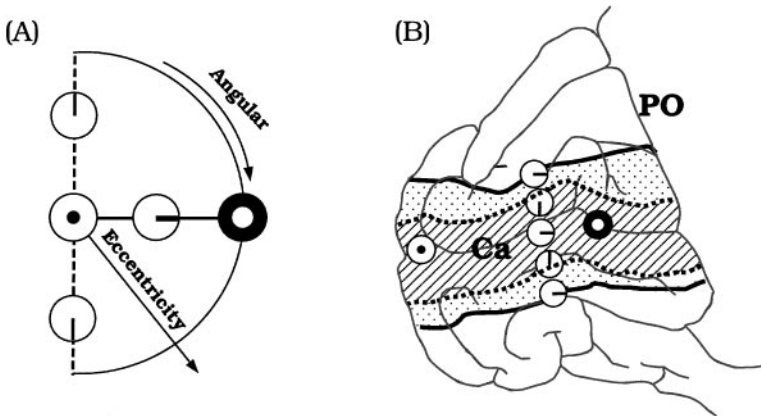


Figure 2 Retinotopic organization of visual areas in the left hemisphere. (A) Icons indicating the visual field positions of the central fixation and periphery (black dot, white surround; white dot, black surround) and the horizontal and vertical meridia (dashed lines) are shown. (B) The approximate positions of areas V1 (hatch marks) and V2 (dotted area) in a sketch of the medial surface of the left occipital lobe are shown. The visual field icons are superimposed on the sketch to indicate the retinotopic organization within areas V1 and V2. The positions of the fundus of the calcarine sulcus (Ca) and parieto-occipital sulcus (PO) are also shown.

A second dimension of retinotopic organization, the angular dimension, is represented on a path that traverses from the lower to the upper lip of the calcarine sulcus. Along this path, the visual field representation shifts from the upper vertical meridian through the horizontal meridian to the lower vertical meridian (see Figure 2*B*). Figure 3*B* represents a flickering wedge that rotates slowly about fixation. This rotating wedge stimulus creates a traveling wave of neural activity that spreads from the lower to the upper lip of the calcarine. Because of the different angular representations in V1 and V2 (see Figure 2*B*), the traveling wave reverses direction at the border. Similarly, although not shown, visual area V3 surrounds V2 and the traveling wave reverses direction again at the V2/V3 border. Hence, measurements using the rotating wedge stimulus (Figure 3*B*) reveal the boundaries between retinotopically organized visual areas.

Traveling Wave Measurements

First, consider a contracting ring stimulus. When it is seen through a small aperture in the visual field, such as the receptive field of a neuron, the visual field alternates between the flickering checkerboard and the neutral gray field. The alternation of the contrast pattern and uniform field causes a waxing and waning of the neural response. If the stimulus moves at a constant velocity from periphery to fovea, the alternation frequency of the response will be the same for all points in the visual field. However, the temporal phase of the response will differ. Neurons with receptive fields in the periphery will respond earlier

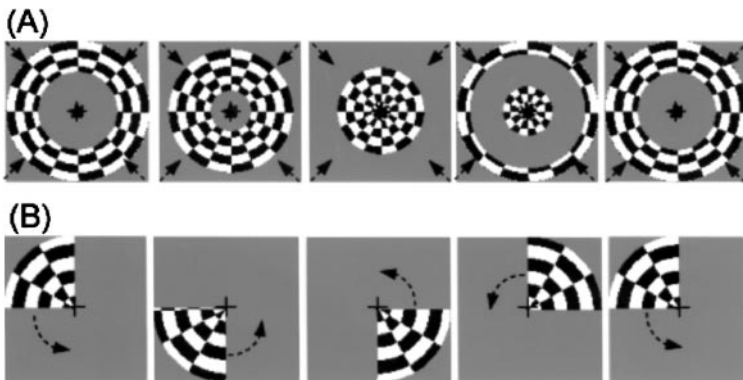


Figure 3 Images of the stimuli used for phase-encoded measurements of retinotopic organization. The contracting ring (*A*) and rotating wedge (*B*) are shown at different moments in time. (*arrows*) The direction of motion of the stimuli; not present in the actual display. These stimuli cause a traveling wave of neural activity to sweep across the cortex in either the eccentricity dimension (*A*) or the angular dimension (*B*).

than neurons with receptive fields near the fovea. Hence, the phase of the response defines the receptive field position along the dimension of eccentricity. Retinotopic mapping methods that rely on this phase signal to map the visual field responses are called phase-encoded.

Figure 4A shows a linear region of interest running from posterior to anterior cortex in an image plane that runs along the fundus of the calcarine sulcus. Figure 4B shows the time course of the fMRI signal at each location along the linear region. One axis of the surface plot represents time, and the second axis represents distance along the region of interest. The time series at each pixel modulates six times, corresponding to the number of periods of the stimulus. The phase of the modulation varies systematically with position in the cortex. The plot shows the traveling wave of neural activity caused by the contracting rings.

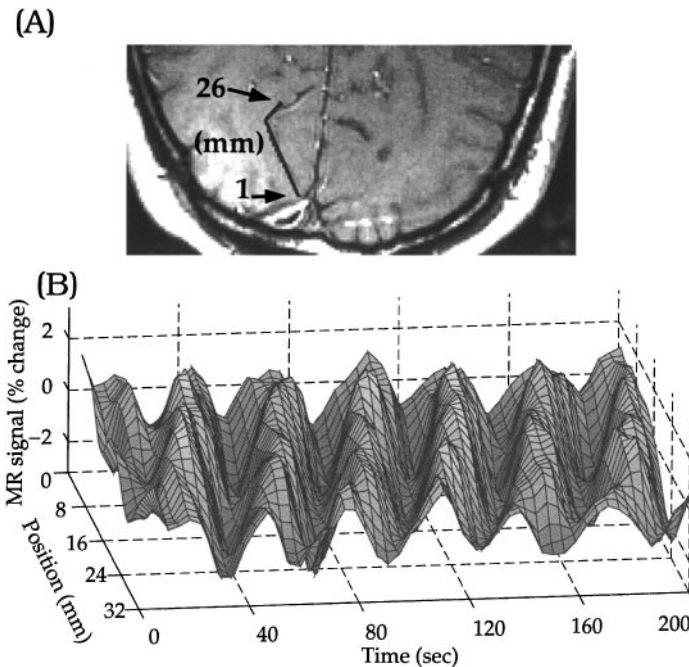


Figure 4 The traveling wave response in primary visual cortex in the left hemisphere caused by a contracting ring stimulus. (A) The magnetic resonance image (MRI) is shown in a plane that runs through the calcarine sulcus. The region of interest, shown by the black line, runs along the calcarine sulcus. (B) The functional fMRI time series at each location within the region of interest is shown. The signal modulates each time the ring passes through a cycle. The phase of the activation in posterior cortex is delayed compared with posterior anterior, creating a traveling wave.

Flattened Cortical Representations

The calcarine sulcus, like most large brain structures, does not stay within a plane over a large distance. To obtain a more complete representation of the activity in area V1, measurements must be integrated from several different images. One way to do this is to take advantage of the fact that neocortical gray matter is much like a folded sheet. Segment the gray matter in a series of image planes and then computational algorithms can be used to unfold the cortical sheet, representing it in a single image. It is also possible to physically unfold macaque and human cortex (e.g. Van Essen & Maunsell 1980, Tootell et al 1983, Gattas et al 1988, Van Essen & Drury 1997). Such representations are useful for understanding the spatial organization of visual areas.

To create flattened representations of human cortex from anatomical MR images, two technical challenges must be met. First, methods are required for identifying the location and contiguity of the gray matter. Teo et al (1998) have developed (and distributed) a method for obtaining a segmented, connected representation from MR images. Figure 5 (see color figure) shows an example of an anatomical image with the regions segmented into white and gray matter. Notice that gray matter on opposite sides of a sulcus can be adjacent within a single image at the 1-mm resolution. Although they touch in the image, the gray matter points are not connected because contiguity is determined by the relationship to the white matter. Unless one correctly determines the contiguity of the gray matter points arising from opposite sides of the sulcus, it is impossible to create accurate flattened representations of the gray matter.

Second, a method is required for converting the representation of the folded, three-dimensional gray matter into a flattened, two-dimensional image. This part of the flattening procedure can be accomplished by specifying the measures within the original (folded) representation that should be preserved and then defining an algorithm to create a flattened representation that preserves these measures. A number of measures have been proposed. Carman et al (1995), Dale & Sereno (1993), and Drury et al (1996) suggest preserving a mixture of measures, including angles and area. Wandell et al (1996) designed and distributed an algorithm to preserve interpoint distances (this method of gray matter segmentation and unfolding can be obtained at <http://white.stanford.edu/wandell.html>).

Figure 6 (see color figure) shows an example of how gray matter from a collection of images was merged into a single picture using the flattening algorithm of Wandell et al (1996). Eight different anatomical images are shown with a color code. The position of the gray matter from each of these planes is indicated in the large image. The locations of major anatomical landmarks are also shown.

By overlaying the measured functional MR activity onto this flattened representation, we obtain a more complete picture of the retinotopic organization

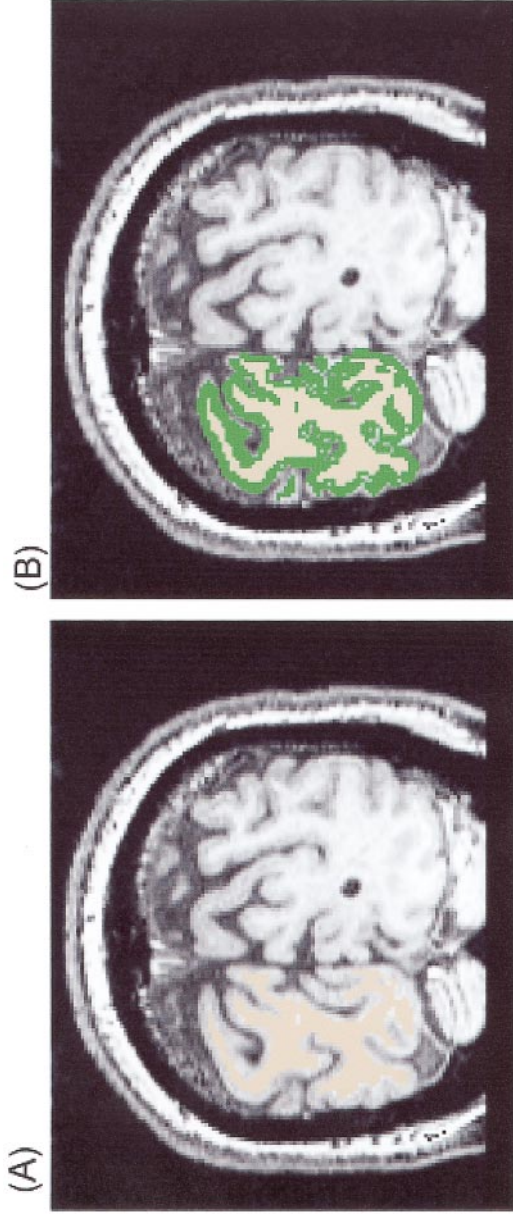


Figure 5 The semiautomatic selection of gray matter from magnetic resonance images. (A) The software identifies the white matter, indicated by the *tan overlay*, based on intensity levels and structural considerations. Notice that the white matter on opposite sides of sulci is well separated. (B) The location of the gray matter is computed by adding gray matter layers onto the white matter (*green overlay*). Gray matter positions on either side of a sulcus can about one another without interfering with the unfolding algorithm because contiguity is determined by the white matter.

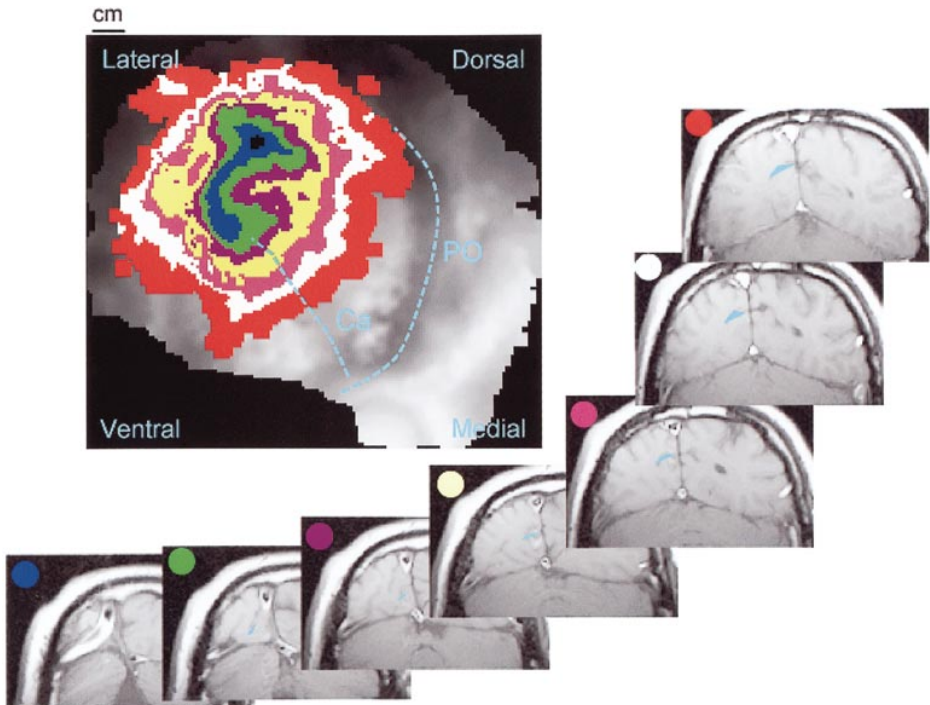


Figure 6 Flattened representation of one occipital lobe. An automatic algorithm transforms the segmented, connected representation of gray matter into an image in which interpoint planar distances are close to the same interpoint distances measured along the cortical surface. The seven small images are anatomical measurements made perpendicular to the calcarine sulcus. The center of the flattened representation is a point at the fundus of the calcarine sulcus in the middle anatomical image. The correspondence between gray matter in each of the seven images and the main image is indicated (*colored overlays*). The *gray-shading* of other gray-matter points, those not in any of the seven measurement planes, indicates the position of the unfolded points with respect to the medial (*light*) to lateral (*dark*) axis of the brain. The location of the fundus of the calcarine (Ca) and the parieto-occipital (PO) sulci are shown in the flattened representation (*dashed cyan lines*).

across the cortical surface. Figure 7 (see color figure) shows an example of phase-encoded responses to an expanding ring stimulus, which is the same as the contracting ring but moving in the opposite direction. The colors code the response phase; each phase is uniquely associated with an eccentricity in the visual field. Comparison of the legend with the colors on the flattened image shows the broad retinotopic organization with respect to eccentricity.

From measurements of responses to expanding and contracting rings, we can estimate how the eccentricity dimension is represented in intact human brains. Engel et al (1994, 1997a) developed a simple formula relating position within area V1 (millimeters from the point representing 10°) to position within the visual field (degree of visual angle):

$$\ln E = 0.63D + 2.303,$$

where E is eccentricity measured in degree from fixation, and D is cortical distance (in millimeters) from the cortical position representing 10° of eccentricity. Cortical locations anterior to that point are assigned positive values, and cortical locations posterior to that point are assigned negative values.

This representation agrees well with estimates obtained using completely different means in monkeys and humans (DeYoe et al 1996, Engel et al 1997a, Horton & Hockina 1997; RBH Tootell, personal communication). In a widely cited paper, Sereno et al (1995) suggested that there were significant differences in cortical magnification between monkey and human striate and extrastriate regions. This observation has not been replicated.

Visual Area Boundaries

The rotating wedge stimulus creates a traveling wave that reverses direction at the boundaries between the visual areas. These reversals occur because of the representation of the angular representation (see Figure 2B). By measuring the locations of the traveling wave reversals using fMRI, the visual area boundaries can be located (Sereno et al 1995, DeYoe et al 1996, Engel et al 1997a).

Figure 8 (see color figure) shows the angular dimension of retinotopic organization on a flattened cortical representation. The colors represent the angular position in the visual field of the rotating wedge that activated the region. The visual area boundaries, derived from phase-encoded fMRI measurements, are placed at locations where the traveling wave reversed direction. For example, starting at the dorsal boundary of V1 and proceeding ventrally, the visual field representation changes from lower vertical midline, to horizontal meridian, to upper vertical midline. Then, at the V1/V2 border, the representation changes direction from vertical midline back to horizontal midline. The traveling wave reverses direction at the V1/V2 border and the boundary is placed at the location of this reversal.

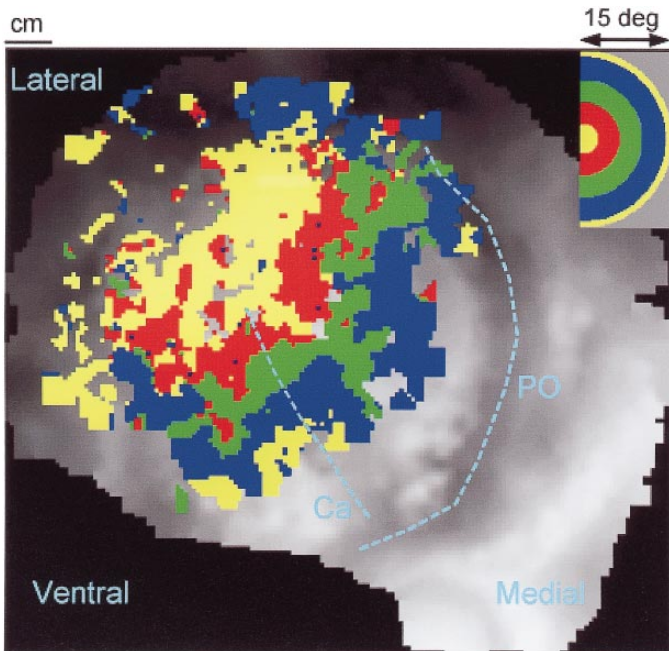


Figure 7 The retinotopic structure of a human brain with respect to eccentricity. The color at each position shows the visual stimulus eccentricity (see *inset*) that evoked activity. Other details as in Figure 6.

Area V1, in calcarine cortex of each hemisphere, represents an entire hemifield. The dorsal and ventral boundaries of V1 are separated by roughly 4 cm and fall on the cortical surface at the upper and lower lips of the calcarine. Area V1 is bordered by two cortical regions, each roughly 1 cm, that form area V2. Dorsal V2 (V2d) represents the lower quarter of the visual field and ventral V2 (V2v) represents the upper visual field.

The strip V2v (V2d) is bounded by another distinct cortical strip called V3v (V3d). Like their neighbors, V3d and V3v each represent one quarter of the visual field, and each spans roughly 1 cm of width and 6–8 cm of length. In macaque, dorsal V3, but not ventral V3, receives projections from V1; dorsal V3, but not ventral V3, has a large minority of directionally selective cells; the anterior border of ventral V3 is demarcated by a strip of callosal inputs that is more precisely organized than the callosal inputs to dorsal V3 (Burkhalter et al 1986, Felleman et al 1997). It is unclear whether these separate quarter field representations (V3d, V3v) should be regarded as one or two areas, so we follow the convention of maintaining separate labels for each of the quarter field representations: V2d, V3d, V2v, and V3v.

An additional retinotopically organized area, V3A, is adjacent to V3d (Tootell et al 1997). Area V3A represents the entire hemifield and has a field representation analogous to area V3A in macaque. Figure 8 shows one more retinotopically organized ventral region, tentatively labeled V4v. Further improvements in the SNR and unfolding methods may well result in the discovery of additional retinotopically organized areas.

The retinotopic organization of human visual areas identified using fMRI are consistent with that described in macaque. We are just beginning to learn whether their functional properties are similar. For example, Tootell et al (1997) have argued that there are important differences with respect to motion selectivity. An important task that confronts us now is to understand the way in which visual information flows and is transformed by neuronal processing in these areas.

MOTION

How are the basic features of the visual world, such as color and motion, represented in the human brain? In this section, I describe three examples of measurements of cortical responses to moving stimuli, measurements that address computational questions, including (a) the distribution of activity in response to moving stimuli, (b) the effect of stimulus contrast and color on responses to moving stimuli, and (c) responses to different types of motion.

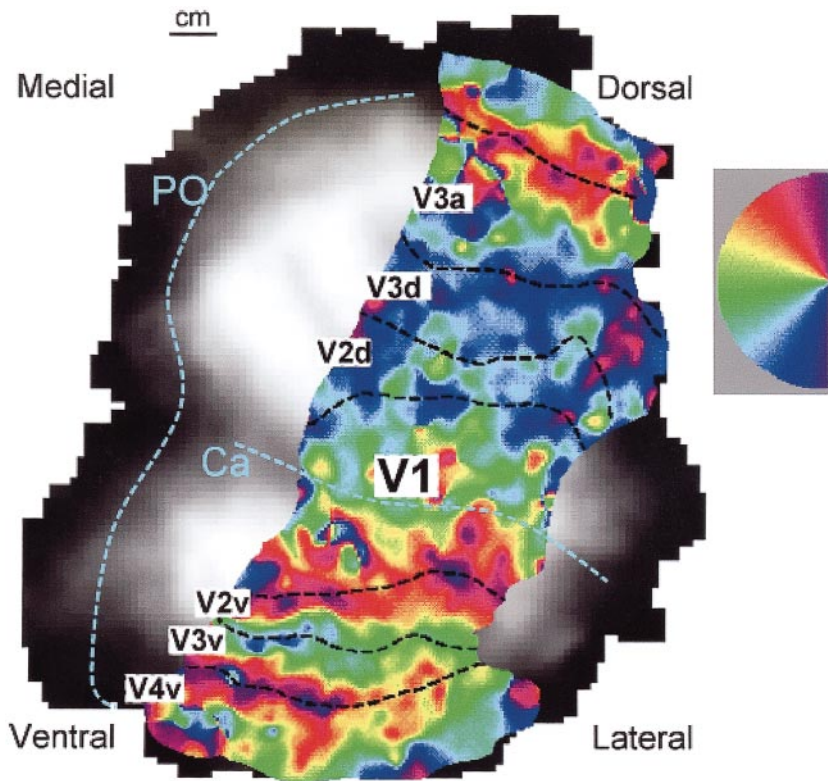


Figure 8 Visual area locations in a flattened representation of one human occipital lobe. The color at each position shows the visual stimulus angular position (see *inset*) that evoked activity. The boundaries between the visual areas are shown (*dashed lines*). Their positions are determined from reversals in the direction of the traveling wave caused by a rotating wedge. See text and Figure 6 for other details.

Motion Responsive Cortex

Using PET and averaging across a group of observers, it is possible to identify a human brain region that is sensitive to moving stimuli (Zeki et al 1991). Using fMRI, it is possible to identify this motion-selective region in individual subjects within a few minutes (Tootell et al 1995).

Figure 9A (see color figure) summarizes the response level in a single image plane roughly parallel but slightly ventral to the calcarine sulcus. The stimulus consisted of a moving field of dots that alternated with a static field of dots every 18 s (response alternation frequency of 1/36 Hz). Figure 9B shows measurements in the same image plane when the stimulus was a flickering checkerboard alternating with a static checkerboard. The color overlay measures the fraction of the power in the signal at the stimulus alternation frequency (scale bar at the right). Activity in the posterior portion of the brain is similar during the two scans. Activity in the lateral anterior region is larger in response to the moving dots than to the flickering checkerboard.

The motion-selective portion of cortex spans several image planes. Figure 9C shows measurements made with the moving dots on a flattened representation of one occipital lobe. Figure 9D shows the responses to the flickering checkerboard. The motion-selective region is near the parieto-occipital junction, roughly 3 cm from foveal representation in posterior V1. The insets show the amplitude of the signal as a function of cycles per scan time in the motion-responsive region. The stimulus was repeated six times during the scan, and the response amplitude² at six cycles per scan is much higher in the presence of motion. There is also significant activity to the flickering checkerboard, but it is reduced in MT+ and not reduced (not shown) in V1. The color map levels are adjusted to emphasize the differences between the two brain regions.

Based on the neuroimaging evidence and anatomical studies of this region in the human brain, it is widely believed that the motion-responsive region contains the human homologue of monkey MT (Zeki et al 1991, Tootell & Taylor 1995). The remaining observation needed to confirm the significance of this region for motion is to demonstrate that the signals are direction selective, as are the single-unit responses in the motion-selective regions of monkey brain. Because the fMRI activity may also arise from adjacent visual areas that are responsive to motion, activity from the motion-selective portion of the brain identified by fMRI is commonly called MT+.

Activity within the motion-responsive region has been confirmed in many laboratories. The most powerful response occurs in primary visual cortex and

²Here and in the following, response amplitude measures the percentage modulation of the fMRI response at the stimulus alternation frequency.

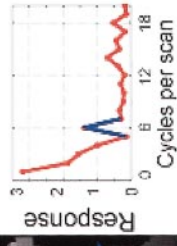
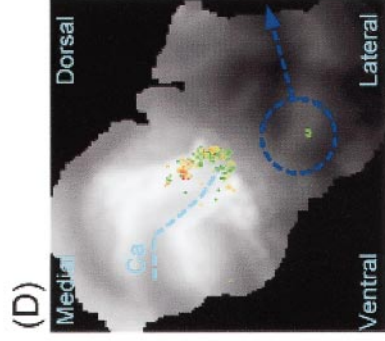
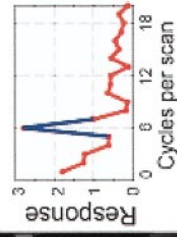
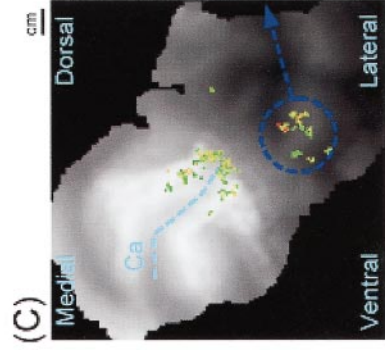
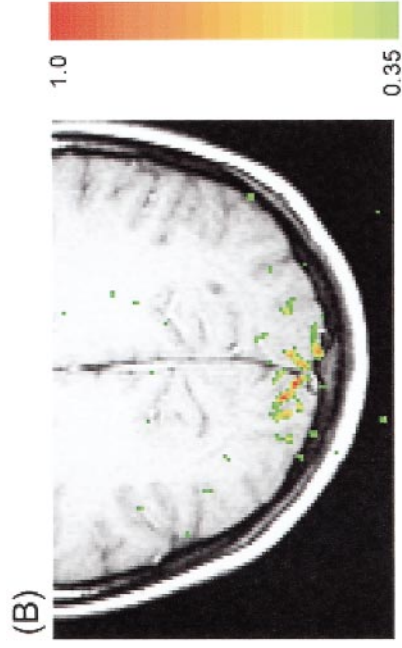
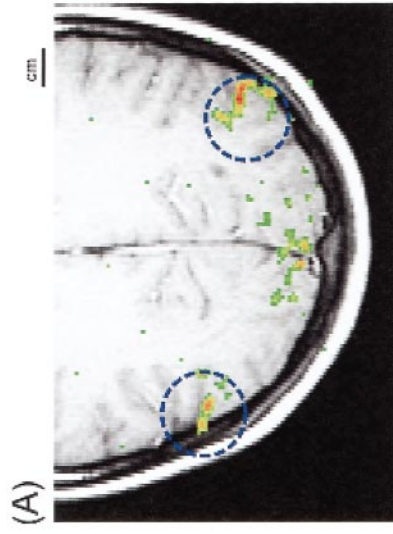


Figure 9 The position of region MT+. (A) (*pseudo-color overlay*) Regions with strong modulation as the observer viewed rapidly moving dots alternating with static dots. There is considerable activity in the posterior brain and on the lateral surface, near the parieto-occipital border (see *circled regions*) in a region that is generally called MT+. (B) When a flickering checkerboard is alternated with a static checkerboard, the MT+ activity is reduced, but activity in the posterior region, near primary visual cortex, is little changed. (C, D) Data in the same two experiments, measured in several planes parallel to the calcarine sulcus, are shown integrated into a flattened representation. The fundus of the calcarine sulcus is shown (Ca). Other details as in Figure 6. (*inset graphs*) The amplitude of the functional magnetic resonance imaging (fMRI) signal in MT+ as a function of temporal frequency for each experiment. The stimulus alternated six times during each experiment, and the *insets* show the increase in the modulation at this frequency. (*color bar*) Measures the temporal correlation between the visual stimulus and the fMRI signal; it applies to all of the images.

MT+, though other portions of the brain respond as well. The strength of the human fMRI response suggests that, as in monkeys, there is a strong signal between primary visual cortex and MT+. The next challenge is to measure the signaling properties of these pathways and to understand their relationship to motion perception.

Motion Contrast-Response Functions

The relatively high SNR of the fMRI signal makes it possible to measure how the response depends on stimulus parameters such as contrast, speed, and color. Figure 10 shows the amplitude of the fMRI signal in MT+ as the subject alternately views a moving, circular, red/green grating for 18 s followed by a uniform field for 18 s. Each point shows the average amplitude measured from six such alternations, spanning 216 s. The horizontal axis shows the grating contrast levels. Using black-white monochrome gratings, reliable MT+ signals can be measured at stimulus contrast as low as 0.5% (not shown). Responses in MT+ to moving patterns saturate at contrast levels as low as 5%, as shown for the red-green pattern in Figure 10. High sensitivity and early saturation have been reported for black-white monochrome gratings (see also Tootell et al 1995).

Figure 10 also shows the contrast-response function in area V1 measured with the same moving target during the same experiment. The response curve in area V1 saturates at roughly four times the MT+ saturation contrast. Tootell et al

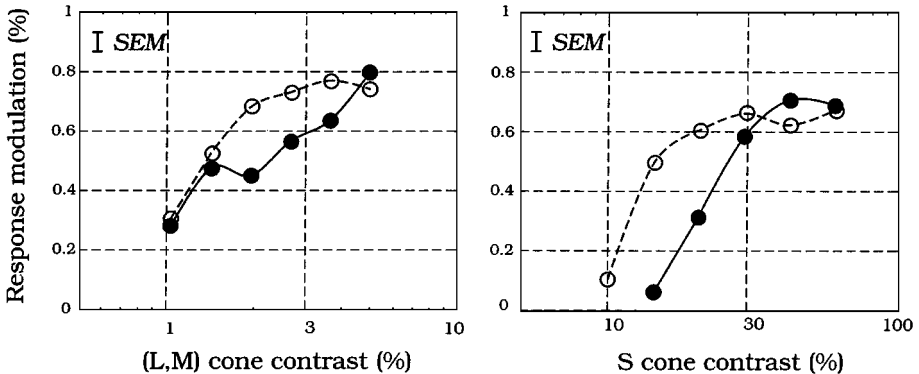


Figure 10 Contrast-response functions measured in area V1 and MT+ using moving gratings. The two panels show measurements made with a moving red/green grating (*left*) and a short-wavelength (S) cone grating (*right*). Curves are the average of measurements in two observers. The response to the red/green grating reaches its maximum level at a very low stimulus contrast, on the order of 5%. Responses to the S-cone grating also saturate, but at stimulus contrasts roughly six times higher, near 30%. L, Long wavelength; M, middle wavelength.

(1995) reported this general relationship, though they report that the response in area V1 saturates at stimulus contrasts that are 15 times greater than MT+.

Why do signals from MT+ saturate at such low contrast levels? The contrast response function to moving targets in area MT+ may be a mechanism that reduces the effect of stimulus contrast on perceived motion. Motion computations should not confound image contrast with image velocity: A low contrast stimulus and a high contrast stimulus, moving at the same velocity, should appear to move at the same velocity. As a general rule, objects do not appear to change speed as they move in front of different backgrounds. Because MT+ responses saturate at low contrast levels, stimulus contrast is generally irrelevant for the computations therein. If we assume that firing rate mainly represents stimulus contrast, then a step-like contrast response function is a computational method of reducing the influence of contrast on motion estimation (Heeger et al 1996, Wandell 1995).

For relatively low contrast levels and for certain colored patterns, stimulus contrast strongly influences perceived speed (Stone & Thompson 1992, Cavanagh & Anstis 1991). One of the most powerful examples of this effect occurs when comparing the speed of a stimulus that excites the short-wavelength (S) cones with another that excites the long- (L) and middle-wavelength (M) cones: The S-cone stimulus has the illusion of moving more slowly than an equally visible (L,M)-cone stimulus. Activity in area MT+ initiated by signals in the S-cones require a much higher contrast level before achieving the same response level as (L,M)-cone signals (Poirson & Wandell 1997) (Figure 10, *right*). The high saturation level for S-cone activity in MT+ may be the source of these contrast-color speed illusions.

Motion and Segmentation

Retinal image motion may arise from different physical causes. One important cause is self-motion: When the observer moves, there is motion in the retinal image. A second source is object-motion: When objects shift their relative positions, there is also motion in the retinal image. Processing of these two types of motion requires analyzing image information in different ways. When the observer moves, coordinated changes occur across a large part of the visual field. But when an object moves, changes are restricted to local image regions. Hence, the processing needed to interpret the two types of motion differ, with respect to the integration of information across the visual field.

These two types of retinal image motion both represent information about objects. When the observer moves, differences in the local motion can be used to identify depth discontinuities, which, in turn, often correspond to object boundaries. Local differences in retinal image motion are also common signs of object boundaries. Because the two types of motion both provide information

about object boundaries, the representation from these two types of motion may be integrated into a single visual account of the scene.

The experiments described up to this point used stimuli with a single motion across the image, much like self-motion. A series of PET and fMRI studies has measured the activity caused by stimuli comprised of two sections moving in different directions, more closely coupled to object-motion (Van Oostende et al 1997, Dupont et al 1997). An example of a stimulus with two moving parts is, say, a circular aperture filled with dots. The dots in the upper half move to the right and the dots in the lower half move to the left. The opposing dot motions leads to the percept of a motion-defined boundary at the contour where the dots motions differ.

There are conflicting reports concerning the responses to moving stimuli that contain a motion-defined boundary. Van Oostende et al (1997; see also Dupont 1997) report that motion-defined boundaries cause substantially more activity than does uniform motion in a region they call kinetic occipital (KO) and whose location, although not known precisely, appears to be somewhat beyond V3A (Van Oostende et al 1997). According to this group, comparison of the responses caused by these stimuli shows significant differences in MT+ but little or no difference in regions near calcarine cortex. Reppas et al (1997) report measurements using similar stimuli and describe significant, retinotopically organized activation in V1, V2, and V3. They do not describe a response in the position corresponding to KO, and they write that “a robust fMRI signal that is selective for motion segmentation...is largely absent from the motion selective area MT/V5 and far extrastriate visual areas” (p. 175). Finally, Mendola et al (1997) report that motion-defined boundaries do cause a significant response in MT+.

Single-unit data suggest that neurons in primary visual cortex should respond to motion-defined boundaries (Chaudhari & Albright 1997). Perhaps more surprising is the small difference between uniform motion and motion-defined boundaries in MT+. Single units in monkey MT are reported to have opponent-surrounds—that is their responses are increased by stimuli with motion-defined boundaries (Allman et al 1985, Born & Tootell 1992).

Although there is no consensus on the activity caused by motion-defined boundaries, there is some agreement on the overall pattern of response to simple moving stimuli. Powerful responses to moving stimuli are found in large regions of the visual cortex. It is likely that motion computations specialized for the different types of motion are parceled out among these different areas. Initial measurements show that the relative size of motion-responses in MT+, V3A, and KO differ depending on the nature of the motion stimulus. Refining the visual stimuli should help reveal how the responses in these different regions work together to form the computational pathways for motion analysis.

COLOR

Color perception results from a sequence of optical and neural computations, beginning in the eye and continuing through the cortex. The initial transformations, and most importantly the absorption of light by the visual photopigments within the L-, M-, and S-cones, are well understood. How the photopigments encode light, and how the photopigment properties can be related to human color-matching, is one of the most complete and satisfying analyses linking brain and behavior in all of neuroscience (Wandell 1995, Ch. 4).

Current computational analyses of color vision seek to explain how appearance, beyond simple matching, can be explained by the properties of retinal and cortical signals. A great deal of perceptual evidence suggests that the central visual pathways represent color signals using an opponent-colors representation comprised of three parallel pathways. The red/green pathway receives opposing L and M signals, and the blue/yellow pathway receives opposing S and L + M signals. The luminance pathway receives L- and M-cone responses of a common sign. The opponent-colors hypothesis helps to explain many perceptual aspects of color vision, including color discrimination and color appearance (Wandell 1995, Ch. 9).

Single-unit studies have revealed possible neural substrates of the opponent-colors signals. Neurons in the retina, lateral geniculate nucleus, and area V1 receive opposing signals from the different cone classes (DeValois et al 1966, Derrington et al 1984, Lennie et al 1990). It has proven difficult, however, to link the response properties of neurons to the perceptual measurements of opponent colors.

Using PET and averaging across a group of observers, Zeki et al (1991) sought to determine whether there is a human brain region that responds particularly strongly to the red/green and blue/yellow opponent-colors dimensions. They compared the PET signal caused by a pair of stimuli. One stimulus, the color image, was a collection of 15 rectangular patches spanning 40° of visual angle. The second stimulus, the monochrome image, consisted of the same collection of rectangular shapes, but the colors were changed to be gray patches luminance-matched to the original, so that the stimuli differed only in their opponent-colors levels. Comparing the activity evoked by the two types of images, Zeki et al report that “the only area showing a significant change of activity was in the region of the lingual and fusiform gyri.” They suggest that the responsive area should be named human V4, based on a proposed homology with macaque V4, an area they believe is specialized for color perception. For the present, I retain the neutral name of VO to refer to the location in ventral-occipital cortex (see also Sakai et al 1995).

The result is puzzling because the data suggest no path for the opponent-colors signals to reach VO; no significant activity is reported in likely sources of this signal, such as V1. One interpretation of these data is that V1 and VO have different opponent-colors responsivities; the opponent-colors signals are amplified in VO compared with V1, similar to the V1-MT relationship for motion.

In contrast to the PET measurements, fMRI measurements demonstrate significant opponent-colors signals in area V1 and V2 (Engel et al 1997b, Kleinschmidt et al 1996, Wandell et al 1998). Figure 11A summarizes the fMRI responses to various colored contrast patterns designed to initiate signals in the L- and M-cones but to be invisible to the S-cones. The stimulus spatial pattern consisted of a flickering, colored checkerboard pattern whose two colors were complementary with respect to a neutral gray background. The checkerboard was alternated with a neutral gray background, and responses were measured at the alternation rate.

To investigate whether the color responses in VO differ from those in V1 and V2, Wandell et al (1998) measured the iso-response curve in that region. They found iso-response curves quite similar to those in V1 (Figure 11B). It appears that the color tuning in VO, measured with simple contrast reversing patterns, is not a unique specialization. Rather, the same color tuning can be measured

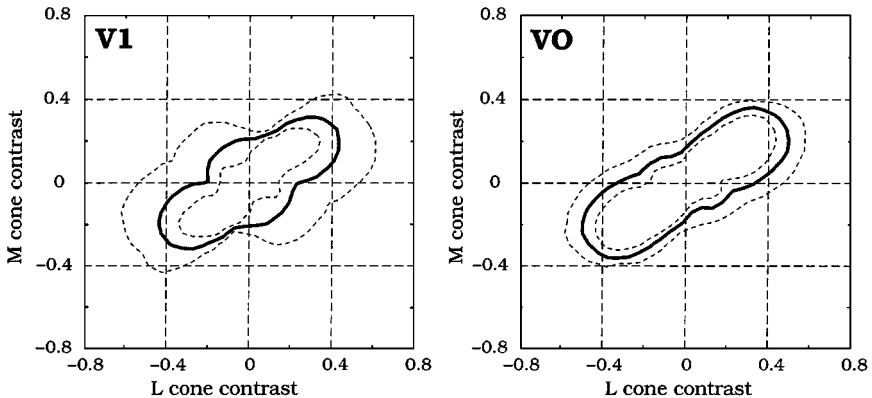


Figure 11 Comparison of the color tuning in area V1 (*left*) and an active region located in the ventral occipital region near the anterior portion of the calcarine sulcus (*right*). (*solid curves*) Stimuli producing an equal functional magnetic resonance imaging response; (*dashed curves*) an 80% confidence interval. Stimuli with opposing long- (L) and middle-wavelength (M) cone contrasts (opponent-colors signals) are about four times more effective at evoking a response than stimuli with covarying L- and M-cone contrasts. The two regions share a common color tuning; other measurements (not shown) suggest that the signal in VO is slightly stronger.

as early as V1. While the responses in V1 and VO were highly correlated, the magnitude of the VO responses were slightly larger. This may be the reason it was possible to identify VO activity, but not the V1 activity, in the PET study (Zeki et al 1991).

The color tuning within a cortical region changes dramatically with the spatiotemporal properties of the visual stimulus (Engel et al 1997b). Hence, the intrinsic color tuning within a cortical region cannot be measured with a single space-time pattern. To appreciate this point, notice that V1 responses to S-cone-driven moving targets are small compared with responses to red/green targets (Figure 10). But, when the stimulus is 1-Hz flickering, V1 responses to S-cone targets are comensurate to L, M-cone targets (Engel et al 1997b). Until shown otherwise, expect that the color tuning within an area depends on the spatiotemporal structure of the stimulus. Differences in color tuning will probably covary with the spatiotemporal structure of the target. This may be a second reason why Zeki et al (1991) failed to detect opponent colors signals in area V1.

As color measurements expand to include more stimuli and cortical territory, it should be possible to measure the distribution of opponent-colors signals across much of the cortical surface. Neuroimaging measurements can complement the information obtained using other methods. Behavioral experiments have proven the importance of opponent-colors signals for visual perception. Single-unit measurements have shown how the cone signals are combined and provided several possible substrates for opponent-colors. FMRI experiments are well suited to analyze activity at the spatial resolution level somewhat finer than areas, and in the next few years columns, for comparing these signals closely with behavioral measurements in individual observers.

BEHAVIOR AND NEUROIMAGING CORRELATIONS

Task Demands

A central goal of vision science is to understand the relationship between neural responses and behavioral performance. Using fMRI, one can acquire neuroimaging and behavioral measurements during the same experimental session, using the same experimental stimuli. The SNR is large enough to permit reliable comparisons between the perceptual and neuroimaging measures in a single observer, without averaging across a population.

One of the most promising observations for linking behavior and neural activity comes from the study of visual attention. FMRI measurements made as an observer alternates between tasks have shown that the fMRI signal fluctuates, even when there is no change in the stimulus (e.g. O'Craven et al 1997,

Beauchamp et al 1997). For example, when subjects view a moving colored stimulus, but alternately respond to questions about the stimulus motion or color, the MT+ signal covaries with the task change. For many experiments, therefore, it is important to control the task demands beyond, say, simple fixation. The large size of the reported fMRI effects are a reason to wonder about the generality of single-unit studies using unconscious, anaesthetized animals.

Dyslexia, Speed Discrimination, and MT+

An important analysis of the relationship between behavior and neuroimaging concerns measurements of individuals with a reading disability, developmental dyslexia. Dyslexics are individuals who have an unexpectedly low reading ability given their intelligence and the absence of other known factors such as lack of motivation, poor learning opportunities, low sensory acuity, or brain injury.

Dyslexics have both phonological and visual defects; for example, they have been shown to perform worse than normal controls in speed discrimination experiments (Lovegrove et al 1980). Livingstone et al (1991) proposed that dyslexic individuals have an abnormality in the magnocellular pathway. In monkeys, this pathway originates with the mosaic of parasol ganglion cells in the retina, projects to a pair of segregated layers in the lateral geniculate nucleus and area V1, and then has a monosynaptic connection to area MT. Several groups have reported behavioral evidence consistent with a magnocellular pathway deficit, in addition to phonological deficits (Lovegrove et al 1980, Livingstone et al 1991, Slaghuis et al 1993), but there have also been failures to support this hypothesis (Victor et al 1993, Hayduk et al 1996).

Data from two neuroimaging studies show that activity in MT+ is significantly lower in dyslexics than in a matched control sample (Eden et al 1996, Demb et al 1997). Because the magnocellular pathway passes through area V1, under appropriate stimulus conditions it should also be possible to find a reduced signal in area V1. Demb et al (1997) (Figure 12) confirmed the three-way correlation between velocity discrimination, reading rate, and fMRI activity in V1 as well as MT+.

A covariation between behavioral and neuroimaging measurements that spans multiple response levels provides a more secure connection than does statistical (binary) classification. The firm association between the neuroimaging and behavioral measurements, spanning many response levels, provides a solid motivation for pursuing the next round of questions concerning the behavioral consequences of the reduced signal (Cornelissen et al 1998) and the biological basis of the reduced signal (Richardson et al 1997).

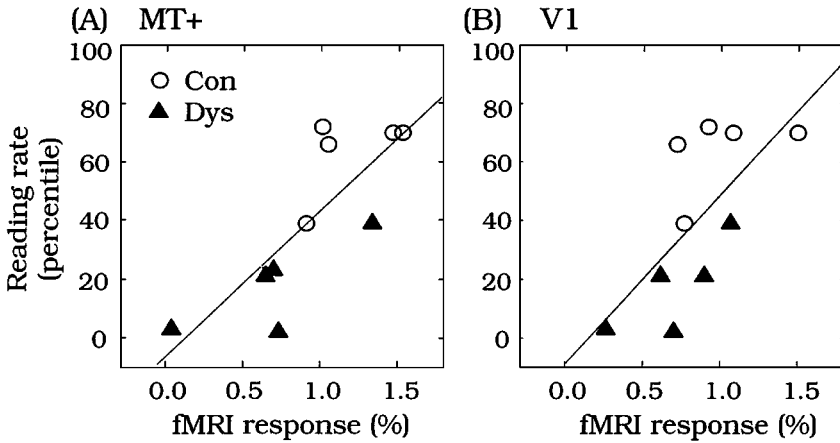


Figure 12 The covariation of relative reading speed and functional magnetic resonance imaging (fMRI) response in two visual areas. Each point shows the fMRI signal and a reading score for a dyslexic subject (*filled triangles*) or a normal control (*open circles*). The stimulus was a rapidly moving ($20^\circ/\text{s}$) sinusoidal grating (0.4 cycles/degree) presented at low (2 cd/m^2) mean luminance. Strong correlations were observed for MT+ activity ($r = 0.80$) and V1 ($r = 0.68$). (Figure provided by J Demb, G Boynton, and D Heeger.)

COMPUTATIONS: PROCESSES AND REPRESENTATIONS

Processes and Representations

Suppose one could measure and predict the real-time response of every neuron in the brain to any stimulus. Would we then understand neural functioning? The computational neuroscientist answers no. In addition to predicting the responses per se, the computational theorist wants to understand the significance of these cortical signals.

Computational questions about cortical signals may be divided into two groups. There are questions concerning information processing, and questions concerning information representation. Some cortical circuits process visual information, transforming it to a form that integrates different types of signals. For example, the visual transformations that correct for changes in the ambient illumination (color constancy) combine information about the local cone absorptions with information about the global illumination. Stereo computations combine two monocular images to compute depth. Processing computations may serve to combine information of different types so that, according to von Helmholtz (1866), we can imagine “such objects” in the visual

field “as would have to be there in order to produce the same impression on the nervous mechanism.”

The result of visual processing must be relayed to other parts of the brain to guide perception and action. Consequently, we should expect that processing results about color, motion, and form are represented at many points in the brain, even though copies of the results may not require further processing.

Some of the differential signals observed in neuroimaging measurements may occur because of processing differences, and others may occur because of representation differences. Consider the computational steps in motion and color perception. As argued earlier, motion processing should not be influenced by the color or contrast of an object, and color processing should not be influenced by motion. Hence, those portions of the brain that perform certain types of motion computations may not contain an accurate representation of stimulus contrast, and for this reason they will not respond differentially to signals with different contrasts. Similarly, there may be portions of the brain that receive information about motion, and other portions that do not.

To understand visual computations, we must bear in mind that the neuronal requirements for different types of processes differ. Motion processing requires an analysis of rapidly varying stimuli (on the order of milliseconds); many essential color computations, such as color constancy, analyze signals that span much longer durations (seconds to minutes). Because the processing demands for color and motion are different, the neural circuits that have evolved to perform these computations might differ as well.

The general requirements for processing and representation may also differ. Processing of color and motion may be separated. It seems likely, however, that the representation of color and motion information may be linked because object representations are likely to coordinate the results of color and motion processing.

Interpreting neuroimaging data as the study of a computational process forces us to consider the flow of visual information. By designing and interpreting neuroimaging experiments in terms of the processes and representations of vision, we obtain a new perspective on the meaning of differences in even simple stimulus comparisons. For example, interpreting color experiments is clarified by referring to opponent-colors computations used in computational models of color vision. Analyses of other perceptual responses, such as motion, also can be clarified by interpreting neuroimaging differences with respect to the computations needed to process and represent motion information. Mechanisms that derive motion selectivity, direction selectivity, and the spatial integration of motion cues are different motion computations that require different representations and processing. The results of some motion computations may flow to eye movement pathways, whereas others may be destined to arrive at object

representations. Understanding the neuroimaging signals caused by various types of motion processing and representations can be carried out only in the context of computational theories. Such computations become an essential tool for interpreting neuroimaging studies, and they will serve to bind neuroimaging measurements to vision science.

Brain Structures and fMRI Resolution

What is the proper spatial scale to search for the computational processes and representations? Over the years, hypotheses have been proposed linking each of the basic spatial scales to visual experience (Parker & Newsome 1998). Barlow (1972, 1995) suggested that the stimulus selectivity measured within single-unit receptive fields identify the perceptual experience associated with that neuron's activity. Mountcastle (1957) demonstrated the significance of columnar organization for the brain, and this principle was exploited in the ground-breaking analysis of the visual pathways by Hubel & Wiesel (1977). Zeki has proposed that perceptual features are segregated by visual areas. Based on a variety of measurements, but most importantly single-unit measurements and human lesion data, Zeki has proposed that V4 is specialized for color and MT/V5 is specialized for motion (Zeki 1991).

Using conventional instruments, the spatial resolution of fMRI yields measurements within the size of many visual areas. Within a few years, the SNR will increase, and it will be possible to resolve activity at the columnar level. Hence, neuroimaging will be able to examine hypotheses about computational mechanisms at two important spatial scales.

Because of the vascular origin of the BOLD signal, the SNR levels will have to increase considerably before the temporal scale of measurement approaches the range of many human behaviors, say a few hundred milliseconds. Current methods for making measurements at fine time scales with fMRI use the same event-related averaging methods used in electrical measurements of neural activity, such as electroencephalography (see, e.g., Buckner et al 1996). It may become possible to use other aspects of the vascular response to measure rapid neural responses. Although the large BOLD signal results from the oversupply of oxygenated blood accumulated over seconds (see Figure 1), there is a brief, localized reduction in the blood oxygen level during the first few hundred milliseconds of neural activity. It is possible to measure this early signal using high (4T) magnetic field strengths, so that it may be possible to obtain finer temporal resolution using fMRI at these levels (Menon et al 1995).

Experimental Design

The studies reviewed here mainly measure how the fMRI signal varies with a stimulus parameter. Different measurements track how the signal varies with

the stimulus position, contrast, color, or motion. These experiments test computational hypotheses about neural activity. In several ways, these computational designs differ from conventional neuroimaging designs, and for this reason it is worth comparing the two types of experimental designs.

CONVENTIONAL DESIGNS Conventional neuroimaging experiments often use the subtraction methodology, which involves the following logical steps. The experimenter defines a pair of conditions that he or she believes differ with respect to a single cognitive or perceptual process. Statistical comparisons are made of the activity in the two conditions, and the neural basis for the putative cognitive process is assigned to the region or regions with significant activity differences.

There are several problems with this research strategy. First, the method includes no means of demonstrating that the differences are due to activity related to the hypothesized cognitive process. Observed differences are ascribed to that process, but there is rarely any further confirmation that the hypothetical cognitive process, rather than some other correlated process, underlies the observed differences (Shulman 1996).

Second, the conclusions drawn from this strategy depend strongly on the quality of the measuring instrument. Oddly, conventional designs are most appealing when used on low-quality instruments because low SNR measurements produce few statistically reliable differences. The poor SNR is advantageous because the results appear most compelling when there is a restricted center of the brain that lights up in response to the putative cognitive process.

As fMRI technology improves, SNR grows. Using the same statistical criterion and repeating experiments with the improved instruments will yield additional sites with reliably different levels of activity. As more responsive sites are identified, a theory based on brain centers becomes untenable. And equally important, localization explanations offer only a minimal account of the computational nature of language, memory, or perception. Localization results, in which a theory means identifying functional centers, do not advance understanding of the computational mechanisms needed to achieve the behavioral results (Zeki 1993, Posner & Raichle 1994).

Conventional subtraction methods are useful for identifying regions of the brain with large responses. But, adhering to an interpretation based on centers is quite likely to result in a theory that will be undermined as the SNR of our instruments improves. Just as the interpretation of the data must consider statistical issues involving different types of errors, so too should we be alert to SNR issues concerning the limits of our instrumentation.

COMPUTATIONAL DESIGNS The fMRI measurements of contrast, color, and motion described above are all differences between a signal and a control,

and in this sense the experiments resemble the conventional approach. But, there are several differences in the methods and these are important to identify.

First, the computational experiments separate the question of localization from the measurements. When color tuning is measured in area V1, or contrast-response functions are measured in MT+, the cortical regions are identified using separate experiments. Second, the computational experiments are not organized around statistical classification methods—does the area light up? The experiments vary an independent parameter (color, contrast, motion) and measure a range of cortical responses that are well above common statistical reliability criteria.

Under low SNR conditions, statistical methods are the primary consideration, and the statistical parameter maps that are widely used in PET and fMRI imaging play a crucial role. But as instrumental SNR improves and measured differences between conditions become much larger than statistical significance, new measurement approaches are required. It is not informative to know that the activity of one pixel is significant to one part in 10^{10} and the adjacent pixel is significant to one part in 10^{11} . These statistical significance levels are related to the measurements through complex nonlinear transformations so that the numerical values are decoupled from the actual measurements. Furthermore, there is no basis for spatial averaging the parameter maps per se as is sometimes done (Reppas et al 1997).

The ability to measure a range of signal levels provides a greater freedom to measure stimulus selectivity properties in various brain regions and to develop computational models of the signal transformations. The conventional design can help us decide where to look first. As the instrument SNR extends the data beyond binary statistical classification, we must apply quantitative techniques and standards of analysis suited to the larger range of measurements.

CONCLUSIONS

For more than a century, scientists have used an enormous variety of methods to analyze the optical, neural, and computational elements of vision. Our field has been open to methods that span questions concerning perception, computation, physiology, and genetics. As we adopt each new method, we establish some consistency with the knowledge we hold secure before we consider accepting findings based on the new method.

In a few short years, we have learned that functional MRI provides a view of the human cortex that is consistent with some of our basic tenets: Early visual cortex is divided into separate, retinotopically organized areas; these areas themselves are divided into ventral and dorsal components; certain regions of the brain are highly responsive to moving stimuli; responses to moving targets

increase with stimulus contrast and saturate at high contrast levels; multiple areas respond, with different relative power, to different types of motion; and opponent-colors signals are present in several cortical areas.

Functional MRI has begun to yield new insights that complement those of single-unit recordings, behavioral measurements, and computational theories. The powerful representation of opponent-colors signals in primary visual cortex and the association between reading and the magnitude of MT+ signals are but two examples. Many more will be found.

fMRI is a new tool for probing the intact, alert, human brain. With this tool, neural activity that has been hidden can now be measured. fMRI provides more direct information about neural computations than can be inferred from behavioral and computational analyses, at useful spatial and temporal resolution. The fMRI measurements fall in a previously unoccupied resolution, between behavior, single-unit recordings, and evoked potentials. We will learn much from this point of view.

ACKNOWLEDGMENTS

I thank H Baseler, GM Boynton, EJ Chichilnisky, JB Demb, DH Heeger, WT Newsome, and AB Poirson. This work was supported by grant NEI EY03164 and a McKnight Senior Fellowship.

Visit the *Annual Reviews* home page at
<http://www.AnnualReviews.org>

Literature Cited

- Allman J, Miezin F, McGuinness E. 1985. Direction- and velocity-specific responses from beyond the classical receptive field in the middle temporal visual area (MT). *Perception* 14(2):105–26
- Barlow HB. 1972. Single units and sensation. *Perception* 1:371–94
- Barlow H. 1995. The neuron doctrine in perception. In *The Cognitive Neurosciences*, MS Gazzaniga. Cambridge, MA: MIT Press
- Beauchamp MS, Cox RW, DeYoe EA. 1997. Graded effects of spatial and featural attention on human area MT and associated motion processing areas. *J. Neurophysiol.* 78(1): 516–20
- Bonhoeffer T, Grinvald A. 1996. Optical imaging based on intrinsic signals: the methodology. In *Brain Mapping: The Methods*, ed. AW Toga, JC Mazziotta. New York: Academic
- Born RT, Tootell RBH. 1992. Segregation of global and local motion processing in primate middle temporal visual area. *Nature* 357(6378):497–99
- Boynton GM, Engel SA, Glover GH, Heeger DJ. 1996. Linear systems analysis of functional magnetic resonance imaging in human V1. *J. Neurosci.* 16(13):4207–21
- Buckner RL, Bandettini PA, O'Craven KM, Savoy RL, Petersen SE, et al. 1996. Detection of cortical activation during averaged single trials of a cognitive task using functional magnetic resonance imaging. *Proc. Natl. Acad. Sci. USA* 93(10):14878–83
- Burkhalter A, Felleman DJ, Newsome WT, Van Essen DC. 1986. Anatomical and physiological asymmetries related to visual areas V3 and VP in macaque extrastriate cortex. *Vis. Res.* 26(1):63–80
- Buxton RB, Frank LR. 1997. A model for the coupling between cerebral blood flow and oxygen metabolism during neural stimulation. *J. Cereb. Blood Flow Metab.* 17(1):64–72

- Carman G, Drury H, Van Essen D. 1995. Computational methods for reconstructing and unfolding the cerebral cortex. *Cereb. Cortex* 5(6):506-17
- Cavanagh P, Anstis S. 1991. The contribution of color to motion in normal and color-deficient observers. *Vis. Res.* 31(12):2109-48
- Chaudhari A, Albright TD. 1997. Neuronal responses to edges defined by luminance vs. temporal texture in macaque area V1. *Vis. Neurosci.* 14:949-62
- Cornelissen PL, Hansen PC, Hutton JL, Evangelinou V, Stein JF. 1998. Magnocellular visual function and children's single word reading. *Vis. Res.* 38(3):471-82
- Dale AM, Sereno MI. 1993. Improved localization of cortical activity by combining EEG and MEG with MRI cortical surface reconstruction: a linear approach. *J. Cogn. Neurosci.* 5:162-76
- Demb JB, Boynton GM, Heeger DH. 1997. Brain activity in visual cortex predicts individual differences in reading performance. *Proc. Natl. Acad. Sci. USA* 94(24):13363-66
- Derrington AM, Krauskopf J, Lennie P. 1984. Chromatic mechanisms in lateral geniculate nucleus of macaque. *J. Physiol.* 357:241-65
- DeValois RL, Abramov I, Jacobs GH. 1966. Analysis of response patterns of LGN cells. *J. Opt. Soc. Am.* 56:966-77
- DeYoe EA, Carman GJ, Bandettini P, Glickman S, Wieser J, et al. 1996. Mapping striate and extrastriate visual areas in human cerebral cortex. *Proc. Natl. Acad. Sci. USA* 93:2382-86
- Drury HA, Van Essen DC, Anderson CH, Lee CW, Coogan TA, Lewis JW. 1996. Computerized mappings of the cerebral cortex: a multiresolution flattening method and a surface-based coordinate system. *J. Cogn. Neurosci.* 8:1-28
- Dupont P, De Bruyn B, Vandenberghe R, Rosier AM, Michiels J, et al. 1997. The kinetic occipital region in human visual cortex. *Cereb. Cortex* 7(3):283-92
- Eden GF, VanMeter JW, Rumsey JM, Maisog JM, Woods RP, Zeffiro TA. 1996. Abnormal processing of visual motion in dyslexia revealed by functional brain imaging. *Nature* 382(6586):66-69
- Engel SA, Glover GH, Wandell BA. 1997a. Retinotopic organization in human visual cortex and the spatial precision of functional MRI. *Cereb. Cortex* 7(2):181-92
- Engel SA, Rumelhart DE, Wandell BA, Lee AT, Glover GH, et al. 1994. fMRI of human visual cortex. *Nature* 369:525
- Engel SA, Zhang X, Wandell BA. 1997b. Color tuning in human visual cortex measured using functional magnetic resonance imaging. *Nature* 388(6637):68-71
- Felleman DJ, Burkhalter A, Van Essen DC. 1997. Cortical connections of areas V3 and VP of macaque extrastriate visual-cortex. *J. Comp. Neuro.* 379(1):21-47
- Felleman DJ, Van Essen DC. 1991. Distributed hierarchical processing in the primate cerebral cortex. *Cereb. Cortex* 1:1-47
- Fox PT, Raichle ME. 1986. Focal physiological uncoupling of cerebral blood flow and oxidative metabolism during somatosensory stimulation in human subjects. *Proc. Natl. Acad. Sci. USA* 83:1140-44
- Fox PT, Raichle ME, Mintum MA, Dence C. 1988. Nonoxidative glucose consumption during focal physiologic neural activity. *Science* 241:462-64
- Gattas R, Sousa APB, Gross CG. 1988. Visuotopic organization and extent of V3 and V4 of the macaque. *J. Neurosci.* 8:1831-45
- Gregory RL. 1974. *Concepts and Mechanisms of Perception*. New York: Scribners
- Hayduk S, Bruck M, Cavanagh P. 1996. Low-level visual processing skills of adults and children with dyslexia. *Cogn. Neuropsychol.* 13(7):975-1015
- Heeger DJ, Simoncelli EP, Movshon JA. 1996. Computational models of cortical visual processing. *Proc. Natl. Acad. Sci. USA* 93:623-27
- Holmes G. 1918. Disturbances of vision by cerebral lesions. *Br. J. Ophthalmol.* 2:353-84
- Holmes G. 1944. The organization of the visual cortex in man. *Proc. R. Soc. London Ser. B* 132:348-61
- Horton J, Hoyt W. 1991. The representation of the visual field in human striate cortex. *Arch. Ophthalmol.* 109:816-24
- Horton JC, Hocking DR. 1997. Relative magnification of the central visual field representation in striate cortex of macaques and humans. *Proc. Soc. Neurosci.* 27:755.11
- Hubel DH. 1988. *Eye, Brain and Vision*. New York: Freeman
- Hubel DH, Wiesel TN. 1977. Functional architecture of macaque visual cortex. *Proc. R. Soc. London Ser. B* 198:1-59
- Kleinschmidt A, Lee BB, Requart M, Frahm J. 1996. Functional mapping of color processing by magnetic resonance imaging of responses to selective p- and M-pathway stimulation. *Exp. Brain Res.* 110(2):279-88
- Kwong KK, Belliveau JW, Chesler DA, Goldberg IE, Weisskoff RM, et al. 1992. Dynamic magnetic resonance imaging of human brain activity during primary sensory stimulation. *Proc. Natl. Acad. Sci. USA* 89:5675-79
- Lai S, Hopkins AL, Haacke EM, Li D, Wasserman BA, et al. 1993. Identification of vascular structures as a major source of signal contrast

- in high resolution 2D and 3D functional activation imaging of the motor cortex at 1.5T: preliminary results. *Mag. Res. Med.* 30:387–92
- Lennie P, Krauskopf J, Sclar G. 1990. Chromatic mechanisms in striate cortex of macaque. *J. Neurosci.* 10(2):649–69
- Livingstone MS, Rosen GD, Drislane FW, Galburda AM. 1991. Physiological and anatomical evidence for a magnocellular defect in developmental dyslexia. *Proc. Natl. Acad. Sci. USA* 88(18):7943–47
- Lovegrove WJ, Bowling A, Badcock D, Blackwood M. 1980. Specific reading-disability: differences in contrast sensitivity as a function of spatial-frequency. *Science* 210:439–40
- Malonek D, Grinvald A. 1996. Interactions between electrical activity and cortical microcirculation revealed by imaging spectroscopy: implications for functional brain mapping. *Science* 272:551–54
- Marr D. 1982. *Vision*. San Francisco: Freeman
- Mendola JD, Dale AM, Liu AK, Tootell RBH. 1997. The representation of real and illusory contours in human visual cortical areas revealed by fMRI. *Proc. Soc. Neurosci.* 27:550.11
- Menon RS, Ogawa S, Hu X, Strupp JP, Anderson P, Ugurbil K. 1995. BOLD based functional MRI at 4 Tesla includes a capillary bed contribution: echo-planar imaging correlates with previous optical imaging using intrinsic signals. *Magn. Reson. Med.* 1995:453–59
- Moseley M, Glover GH. 1995. Functional MR imaging: capabilities and limitations. In *Functional Neuroimaging*, ed. J Kucharczyk, M Moseley, T Roberts, W Orrison. North American Imaging Clinics
- Mountcastle VB. 1957. Modality and topographic properties of single neurons of cat's somatic sensory cortex. *J. Neurophysiol.* 20:408–34
- O'Craven KM, Rosen BR, Kwong KK, Treisman A, Savoy RL. 1997. Voluntary attention modulates fMRI activity in human MT-MST. *Neuron* 18(4):591–98
- Ogawa S, Tank D, Menon R, Ellermann J, Kim S, et al. 1992. Intrinsic signal changes accompanying sensory stimulation: functional brain mapping with magnetic resonance imaging. *Proc. Natl. Acad. Sci. USA.* 89:5951–55
- Parker AJ, Newsome WT. 1998. Sense and the single neuron. *Annu. Rev. Neurosci.* 21:227–77
- Poirson AB, Wandell BA. 1997. Color tuning to moving stimuli in the human visual cortex measured using fMRI. *Proc. Soc. Neurosci.* 27:550.5
- Posner MI, Raichle ME. 1994. *Images of Mind*. New York: Freeman
- Reppas JB, Niyogi S, Dale AM, Sereno MI, Tootell RBH. 1997. Representation of motion boundaries in retinotopic human visual cortical areas. *Nature* 388(6638):175–79
- Richardson AJ, Cox II, Sargentoni J, Puri BK. 1997. Abnormal cerebral phospholipid-metabolism in dyslexia indicated by p-31 magnetic-resonance spectroscopy. *NMR Biomed.* 10(7):309–14
- Sakai K, Watanabe E, Onodera Y, Uchida I, Kato H, et al. 1995. Functional mapping of the human colour centre with echo-planar magnetic resonance imaging. *Proc. R. Soc. London Ser. B* 261(1360):89–98
- Sereno MI, Dale AM, Reppas JB, Kwong KK, Belliveau JW, et al. 1995. Borders of multiple human visual areas in humans revealed by functional MRI. *Science* 268:889–93
- Shulman RG. 1996. Interview with Robert G Shulman. *J. Cogn. Neurosci.* 8(5):474–80
- Slaghuys WL, Lovegrove WJ, Davidson JA. 1993. Visual and language processing deficits are concurrent in dyslexia. *Cortex* 29:601–15
- Stone LS, Thompson P. 1992. Human speed perception is contrast dependent. *Vis. Res.* 32:1535–49
- Teo P, Sapiro G, Wandell BA. 1998. Creating connected representations of cortical gray matter for functional MRI visualization. *IEEE Med. Trans.* 16:852–63
- Tootell RBH, Mendola JD, Hadjikhani NK, Ledden PJ, Liu AK, et al. 1997. Functional analysis of V3A and related areas in human visual cortex. *J. Neurosci.* 17(18):7060–78
- Tootell RBH, Reppas JB, Kwong KK, Malach R, Born RT, et al. 1995. Functional analysis of human MT and related visual cortical areas using magnetic resonance imaging. *J. Neurosci.* 15:3215–30
- Tootell RBH, Taylor JB. 1995. Anatomical evidence for MT and additional cortical visual areas in humans. *Cereb. Cortex* 1:39–55
- Tootell RGH, Silverman MS, DeValois RL. 1981. *Science.* 214(813)
- Van Essen DC, Drury HA. 1997. Structural and functional analyses of human cerebral cortex using a surface-based atlas. *J. Neurosci.* 17(18):7079–102
- van Essen DC, Maunsell JH. 1980. Two dimensional maps of the cerebral cortex. *J. Comp. Neurol.* 191:255–81
- Van Essen DC, Zeki SM. 1978. The topographic organization of Rhesus monkey prestriate cortex. *J. Physiol.* 277:193–226
- Van Oostende S, Sunaert S, Van Hecke P, Marchal G, Orban GA. 1997. The kinetic occipital (KO) region in man: an fMRI study. *Cereb. Cortex* 7(7):690–701

- Victor JD, Conte MM, Burton L, Nass RD. 1993. Visual-evoked potentials in dyslexics and normals: failure to find a difference in transient or steady-state responses. *Vis. Neurosci.* 10(5):939–46
- von Helmholtz H. 1866. *Physiological Optics*. Transl. JP Southall, 1911. Washington, DC: *Opt. Soc. Am.* (From German)
- Wandell BA. 1995. *Foundations of Vision*. Sunderland, MA: Sinauer
- Wandell BA, Baseler H, Poirson AB, Boynton GM. 1998. Computational neuroimaging: color tuning in two human cortical areas measured using fMRI. In *Color Vision: From Molecular Genetics to Perception*, ed. K Gegenfurtner, T Sharpe. Cambridge, UK: Cambridge Univ. Press. In press
- Wandell BA, Engel SA, Hel-Or HZ. 1996. Creating images of the flattened cortical sheet. *Invest. Ophthalmol. Vis. Sci.* 37:S1081
- Zeki S. 1993. *A Vision of the Brain*. Oxford, UK: Blackwell Sci.
- Zeki S, Watson JDG, Lueck CJ, Friston KJ, Kennard C, Frackowiak RSJ. 1991. A direct demonstration of functional specialization in human visual cortex. *J. Neurosci.* 11(3):641–49
- Zeki SM. 1969. Representation of central visual fields in prestriate cortex of monkey. *Brain Res.* 14:271–91